Design, Validation, and Characterization of CERN's SpaceRadMon-NG CubeSat Payload for Space Radiation Monitoring Missions

JASPER DIJKS
ALESSANDRO ZIMMARO
ENRICO CHESTA
SALVATORE DANZECA
RUDY FERRARO
RUBÉN GARCÍA ALÍA, Member, IEEE
PANAGIOTIS GKOUNTOUMIS, Member, IEEE
ALESSANDRO MASI
European Organization for Nuclear Research (CERN), Geneva, Switzerland

ALESSANDRA MENICUCCI
TU Delft Space Systems Engineering (SpE), GB, Delft, Netherlands

JEFFREY PRINZIE, Member, IEEE
KU Leuven Electrical Engineering (ESAT), Geel, Belgium

Understanding and monitoring the space environment is of great importance for the design and development of space avionics. This is especially critical when employing radiation-sensitive commercial-off-the-shelf (COTS) components in space systems. This work presents the design, validation, and characterization of the SpaceRadMon-NG radiation monitoring payload and its sensors, a modular system built around such components. The study covers the payload configuration and preparations for the radiation effects during the in orbit flight experiment (RADIOX) mission, part of the SYNDEO-1 CubeSat. Unique methodologies were applied for radiation qualification, system-level validation and sensor characterization to ensure reliable operation in space. The payload features enhanced capabilities compared to the previous version, including improved resolution, power efficiency, and system modularity. Mechanical and radiation tests confirmed system robustness, and a cross-section smaller than $8.58{\cdot}10^{-12}$ cm^2 was determined at a 95% confidence level. Sensor performance was excellent, with relative errors of 0.65% for the COTS static random access memory and 0.41% for the floating gate dosimeter (FGDOS) compared to reference devices. A novel FGDOS characterization under simultaneous temperature cycling and irradiation confirmed the stability of its temperature coefficient and identified an effective compensation method using a radiation-insensitive reference sensor. This compensation approach can be extended to other radiation-sensitive components in space. With its successful validation in space-representative environments, the payload is ready for in-orbit demonstration, where it will measure the total ionizing dose and high energy hadron fluence in low Earth orbit.

Received 6 February 2024; revised 17 April 2025; accepted 16 July 2025. Date of publication 6 August 2025; date of current version 8 December 2025.

DOI. No. 10.1109/TAES.2025.3595559

Refereeing of this contribution was handled by Giancarmine Fasano.

Authors' addresses: Jasper Dijks was with CERN, Geneva, CH-1211 23, Switzerland. He is now with NLR, Amsterdam, 1059 CM, The Netherlands. E-mail: (jasper.dijks@nlr.n); Alessandro Zimmaro, Enrico Chesta, Salvatore Danzeca, Rudy Ferraro, Rubén García Alía, Panagiotis Gkountoumis, and Alessandro Masi are with the European Organization for Nuclear Research (CERN), 1217 Geneva, Switzerland. E-mail: (alessandro.zimmaro@cern.ch, enrico.chesta@cern.ch, salvatore.danzeca@cern.ch, rudy.ferraro@cern.ch, ruben.garcia.alia@cern.ch, panagiotis.gkountoumis@cern.ch, alessandro.masi@cern.ch); Alessandra Menicucci is with the TU Delft Space Systems Engineering (SpE), 2600 GB Delft, The Netherlands. E-mail: (a.menicucci@tudelft.nl); Jeffrey Prinzie is with the KU Leuven Electrical Engineering (ESAT), 2440 Geel, Belgium. E-mail: (jeffrey.prinzie@kuleuven.be). *(Corresponding authors: Jasper Dijks; Alessandro Zimmaro.)*

I. INTRODUCTION

Space radiation has an enormous effect on the design considerations of spacecraft systems and space missions. The space radiation environment must be understood and accurately modeled [1]. This understanding of the environment is fundamental in the assessment of radiation effects on the avionics on-board a spacecraft or satellite and for ensuring radiation hardness assurance (RHA) to space missions [2], [3]. Radiation physics studies and space weather studies are possible additional scopes of characterizing the space environment [4], [5], [6]. In recent years, several CubeSat and small satellite missions have demonstrated effective in-situ monitoring of the space radiation environment using compact instrumentation and student-developed platforms [7], [8], further enabling distributed and cost-effective space weather observations.

Various attempts for creating modular monitoring devices for higher energy particles have been made, which are based on advanced radiation detectors and could be adapted for space applications [9], [10], [11]. Cheaper detectors based on commercial-off-the-shelf (COTS) have also been developed that can measure relatively high energy particles based on the single event upsets (SEU) or single event latch-ups (SEL) in the device [12], [13], [14], [15], [16]. For measuring the total ionizing dose (TID), current state-of-the-art modules are based on a metal-oxide semiconductor field effect transistor (MOSFET) devices such as the radiation sensitive MOSFET (RADFET) [17]. As such, the European Organization for Nuclear Research (CERN) currently heavily relies on RADFETS for TID measurements [18]. CERN is now performing investigations on a new type of radiation sensor that uses a floating gate transistor as the radiation sensitive part: a floating gate dosimeter (FGDOS) [19]. Due to its enhanced radiation monitoring resolution compared to current state-of-the-art sensors, it can improve current capabilities in space radiation monitoring. Its operation is already demonstrated in a lunar fly-by mission [20].

In recent years, CERN has developed a deep understanding of radiation monitoring due to the harsh environment of the large hadron collider (LHC). In particular, developing and qualifying COTS-based monitoring systems that are deployed in mixed-field radiation environments. It now extends this knowledge to radiation monitoring in space, by sending a newly developed and low power payload to space with high-resolution in radiation monitoring. The 1U-CubeSat CERN latchup and radmon experiment student satellite (CELESTA) was developed in the period between 2016 and 2020. It was based on CERN qualified COTS components and has been qualified and validated in CERN high energy accelerator mixed-field facility (CHARM) [21], [22]. After the satellite launch in July 2022 [23], containing the first version of the SpaceRadMon, three limitations to the satellite and payload were identified, which have now been improved in the next generation payload.

One of the limitations of the payload in the satellite was the RADFET, whose resolution was not high enough for the requirements that were set. A second limitation is the measurement of the higher energy particles. A phenomenon that is known as "error bursts" exists on the CY62157EV30LL SRAM, resulting in a rapid increase in the amount of SEUs measured by the sensor. The bursts were caused by micro-latchups generated in the die during the process of reading and writing. This phenomenon was observed in previous studies [24], [25], [26] where a mitigation scheme has been proposed, however, this technology was not mature enough to deploy during the development of CELESTA. Hence, this mitigation proposal was not yet implemented for this mission. Apart from those two limitations, the challenge of power consumption has also been improved in the new payload. The improved lower power consumption makes the system more versatile for longer term missions and has a positive impact on the system's lifetime. An extremely low-power payload was developed by CERN specifically for these characteristics and to increase the knowledge on this topic.

Based on current state-of-the-art improvements and experience gained from the CELESTA mission, CERN is now preparing for the next mission related to monitoring radiation effects in space. The SpaceRadMon-NG is a modular CubeSat payload that will fly on a low Earth orbit (LEO) mission called radiation effects during in orbit flight experiment (RADIOX) mission, part of the SYNDEO-1 satellite operated by ISISPACE. The sensors and components used on the payload are mainly COTS. The payload will measure the TID using the FGDOS and the high energy hadron (HEH) fluence using CY62157EV30LL and IS61WV204816BLL COTS static random access memories (SRAM). Specifically for this mission, the payload's sensor board is equipped with experimental custom 180 nm complementary MOS (CMOS) SRAM devices allowing adjustable sensitivities that will be used to measure the HEH fluence [27]. In future missions, this can be adjusted to other sensors due to the payload's modularity. This article will present a new generation payload solution with enhanced low-power requirements and sensitivity in radiation monitoring. After a first description of the hardware and firmware, there will elaborate on the novelty of overcoming CELESTA limitations. Subsequently, the qualification and validation campaigns performed are explained, of which the methodology can be extended to any type of payload, CubeSat, or smaller satellite. Finally, the methods and results of a new characterization of the FGDOS in a space-like environment will be discussed.

TABLE I
Characteristics of the SpaceRadMon-NG Payload for the RADIOX Mission Configuration Compared to the Previous Version of the Payload

Characteristic	SpaceRadMon-V2	SpaceRadMon-NG
Tolerance [Gy]	250	>418
Power consumption [mW]	165	63.5 (idle), 45.0 (sleep)
Mass [g]	60	57.5
Size [mm]	96.00 × 92.00 × 18.10	96.00 × 92.00 × 16.56
TID sensor	RADFET	FGDOS
Resolution [mGy]	57	2
SRAM sensors	1 SEU, 2 SEL	2 COTS SEU, 2 custom SEU
Voltage monitoring	No	Yes
Temperature monitoring	Yes	Yes
Communication protocol	I^2C	I^2C

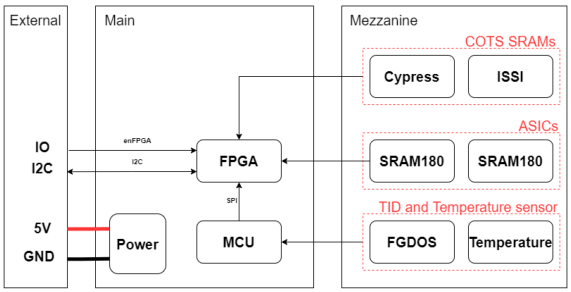

Fig. 1. High level flow diagram of the SpaceRadMon-NG payload's main components for the RADIOX mission configuration. The power requirements are as follows: the FPGA operates at 1.2 and 3.3 V, the MCU and COTS SRAMs at 3.3 V, the ASIC SRAMs between 0.4 and 2.2 V (adjustable), and both the FGDOS and temperature sensor at 5 V.

II. PAYLOAD ADVANCEMENTS

Compared to the current state-of-the-art sensors and experience gained from the CELESTA mission, certain solutions have been implemented on the new payload. In the following paragraphs, the novelty in terms of hardware and firmware will be presented. It will allow the platform to guarantee stricter low-power requirements, improved reliability, and enhanced sensor performance. The characteristics of the payload are summarized in Table I, where the new payload version for the RADIOX mission is compared to the previous version of the SpaceRadMon.

A. Hardware

The system design has been divided into two separate modules, the main-board and the sensor-board. This design was chosen rather than a single board, to increase system versatility. This allows for an easy exchange of the sensor-board, ensuring high flexibility with changing mission requirements with easy integration. The high-level flow diagram of the payload can be seen in Fig. 1, where the two boards and their main components are depicted.

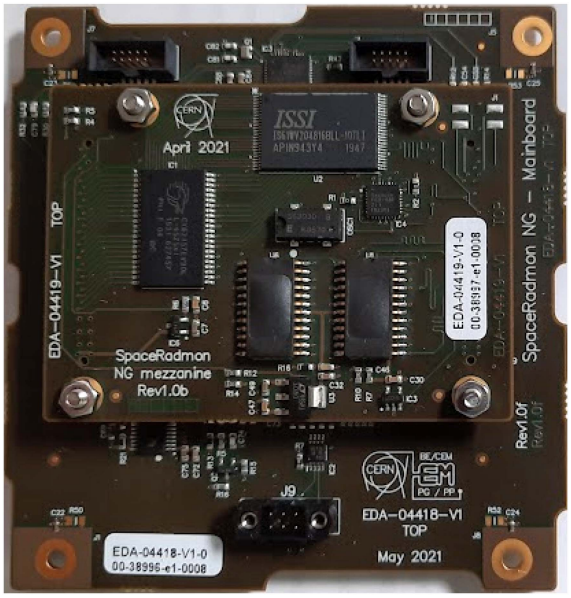

Fig. 2. Photograph of the SpaceRadMon-NG payload from the top for the RADIOX mission configuration.

A photograph of the actual payload can be seen in Fig. 2, showing the stacked boards.

As depicted in Fig. 1, the different voltages required by the system are provided by a power distribution subsystem consisting of different power regulators. The core of the system is a low-power COTS field programmable gate array (FPGA) by Microchip, namely the ProASIC 3 L. It features the possibility of clock gating its internal design through the toggling of a single pin, which can significantly reduce the dynamic power consumption of the overall system. The FPGA interfaces directly with some of the sensors and the microcontroller unit (MCU) [28]. This combination represents one of the major novelties with respect to the payload on CELESTA: the discrete analog-digital converter (ADC) has been replaced by a low-power, high-performance ARM Cortex-M0+ 8-bit-based flash MCU. The MCU contains an embedded ADC, guaranteeing higher radiation tolerance, low-power mode capabilities, and even higher flexibility. Thanks to the different peripherals embedded, it can easily interface with any sensor type, resulting in more freedom when designing the sensor board. This is an improvement over the previous design, where resource constraints on the FPGA limited the design options of the sensor board, reducing the versatility. The use of both an FPGA and an MCU allows an optimal distribution of tasks: the FPGA handles high-speed, parallel sensor interfacing and memory sensor access (e.g., for the SRAM burst detection), while the MCU provides low-power serial interfacing, mixed-signal sensor readout, ADC functionality and supervisory control. This hybrid architecture balances flexibility, power efficiency and robustness in a radiation-tolerant design. At the same time, the lower cross-section of an FPGA, compared to a microprocessor, ensures higher dependability during operation without the need for external intervention. This solution allows the use of more sensitive parts, such as microcontroller units (MCUs), in radiation-prone environments without compromising system performance.

The default sensor board contains two COTS SRAM devices (CY62157EV30LL and IS61WV204816BLL) and two custom slots. For the RADIOX mission, these slots will be filled by two custom SRAM devices (developed at KU Leuven with adjustable voltages of 0.4, 0.8, 1.8, or 2.2 V for adjustable sensitivities). Additionally, there is an FGDOS chip (FGD-03F-Z) and one temperature sensor. The FPGA on the main board interfaces directly with the COTS SEU sensors (SRAMs) and the custom slots, whereas the interfacing to the FGDOS and temperature sensor is performed through the MCU. The payload communicates externally with the satellite mainframe using the I2C protocol. On the same connector, another two available pins are used to provide the 5 V input and the clock gating.

The power consumption of the payload was measured after system integration using a laboratory source/measure unit (SMU) with logging capabilities and external current sensing, under mission-representative operation. Measurements were taken during idle and power-save modes, resulting in 63.5 and 45.0 mW, respectively. These figures reflect real hardware performance, including the operation of all sensors and communication interfaces.

B. Firmware

The firmware of the payload is divided between the FPGA and C-code on the MCU. The firmware architecture on the FPGA is structured by means of finite state machines (FSM). The following FSMs are implemented in the FPGA for RADIOX: main controller, MCU controller, SRAM controller, SRAM180 controller, Flash-Freeze management, SPI, and I2C. The main controller serves as the central FSM, initiating SPI communication to the MCU and taking care of memory readout operations. It acts as an event handler and synchronizer, coordinating the activity of the other FSMs based on system states and external triggers. The MCU controller manages the data retrieval of the FGDOS, temperature and voltage sensors on the payload and sends them to the implemented SPI block. The SRAM controller manages the data acquisition of the CY62157EV30LL and IS61WV204816BLL sensors. The SRAM180 controller takes care of the data retrieval of the custom SRAMs by KU Leuven. This controller can be exchanged for another one when there are different sensors. The flash-freeze management handles the sleep mode of the FPGA to save power. The SPI and I^2C modules are used to take care of the communication between the MCU and FPGA, as well as between the FPGA and the external on-board data handling (OBDH) computer.

Various mitigation techniques have been implemented on the FPGA. The triple modular redundancy (TMR) mitigation technique is applied to both registers and internal RAM to keep the core radiation tolerant; it was automatically deployed by a commercial synthesis tool and verified with proton radiation tests during the prototype phase. Libero from Microchip was used for the synthesis

and implementation of TMR. Additionally, a burst detection firmware was implemented for the CY62157EV30LL SRAM to mitigate SEU bursts in the sensor. This burst detection firmware was based on a previous proposal for the RadMon V6 [25] and has been implemented using alternating block addressing. When a location of the memory is addressed to check for a burst, the rest of the SRAM is kept in data retention and held at a lower voltage than the operating one. Linear addressing is used where blocks are constantly switched, therefore, memory cells are alternatively active and under less stress. This reduces the effective duration of micro-latch-ups and prevents another phenomenon known as "column SEU bursts" seen in a previous study [29] caused by the induced cell stress due to the detection algorithm implemented. Assuming the set of SRAM blocks B_n where n = 0...63, the memory was divided into a left part n = 0...31 and a right part n = 32...63. Starting from the first block, the SRAM is accessed in an alternating manner, giving two detection windows. When the SEU threshold set is reached in one of the detection windows, a burst is detected. The modifications to the algorithm give an increase of 5% of the FPGA resources, which is acceptable for the mitigation it brings. In addition, the disabling of the detection window after detection is turned off allows for full scanning of the memory.

The MCU applies the same mitigation techniques used in the BatMon application [30] to guarantee higher reliability under radiation and, in the event of certain types of failure, to be able to restore the full settings of the MCU without FPGA intervention, such as an internal software watchdog based on the real-time clock peripheral and protection against misconfiguration of critical peripherals [31]. When an error occurs that cannot be detected by these mitigation schemes, the FPGA resets the device acting as an external watchdog. To mitigate SEEs in the MCU SRAM without impacting the performances, software TMR is applied to critical variables such as measurements. For the latter, they are stored in the MCU's internal flash memory to ensure greater reliability under radiation and to prevent loss of information in the event of a reset or power cycle.

III. PAYLOAD QUALIFICATIONS

This section will elaborate on the payload qualifications that have been performed to ensure its operation once in orbit, elaborating on the methods used and the results obtained. The tests performed were a series of mechanical and screening tests by KU Leuven, and radiation tests according to RHA procedures [32], [33] by CERN. The qualification procedures will also demonstrate the functionality of the device in operational-like environments, meaning that if the qualifications pass, the device will be mature enough for its next step: demonstration in orbit during two missions.

A. Mechanical

Screenings have been performed for the system to ensure durability and reliability during missions, such as thermal cycling, electromagnetic compatibility (EMC), and shock and vibration tests. During testing, both structural integrity and electronic functionality were monitored using a built-in self test.

During thermal cycling, the system was cycled from −20 °C to 50 °C. In total, five cycles were performed. These operating temperatures resemble the mission temperature profile in orbit with additional margin.

Vibration tests were performed at the KU Leuven Noise and Vibration Research Lab (LMSD). The test requirements were defined by Arianespace based on the expected vibrations of the Vega-C launcher. The electromagnetic shaker can provide open loop and closed loop stimuli and has system identification to reduce any system/mass related impact. The shaker is 1-D so all tests were repeated for each axis. An accelerometer is mounted on the frame to monitor the acceleration and provide feedback to the vibration loop controller. At the end of the vibration tests, an additional visual inspection was performed on the payload to check for loosening of the bolted connections. A first test was performed to survey the first resonance frequency of the payload. The measured frequency range was 5 to 2000 Hz. The lowest resonance peak was measured at 343 Hz. Sine vibration from 5 to 125 Hz was performed as well as random vibrations up to 14.1 GRMS. Additionally, 15 G sine bursts and 500 G shock tests have been performed. Each axis was evaluated independently. No electronic nor mechanical failures were observed after the mentioned tests.

EMC qualification was performed at KU Leuven FMEC lab in Brugge, according to the MIL-STD-461 G standard. Conductive emission results pass the CE102 specification with a maximum emission of 53 dbμV. Radiative emission measurements initially did not meet the RE102 mask at 24 MHz. This is the third harmonic of the main system clock (8 MHz). After debugging the test setup using handheld electromagnetic interference (EMI) analyzers, it was found that the 3 m power cables were causing the radiative emissions and not the payload. The tests were repeated with a short supply cable of 20 cm, instead of the initial 3 m. The emission was then significantly reduced and fell well within the RE102 mask. Such wiring is also realistic in the final payload. Radiative immunity was verified by emitting towards the payload according to the RS103 specification. During these tests, a self-check is performed to validate if the payload functions properly. During the test, a probe was placed next to the payload to verify the emitted power real-time. The payload functioned nominally without any abnormal behavior.

B. Radiation

Different approaches to RHA of electronics systems for space applications have already been proven successful [34], [35]. For this application, CERN's general RHA procedures are applied to ensure operation in space [32]. It involves two levels of radiation qualification, first for components and subsequently on a system-level. Component screening is carried out at the Proton Irradiation Facility (PIF) of the Paul Scherrer Institute (PSI) using a 200 MeV

proton beam. This screening process is only passed by components that meet the initial system requirements set of 500 Gy. In the case of SpaceRadMon-NG, this qualification phase was facilitated due to the components radiation testing during CELESTA preparations, which met the system requirements. Additionally, the new MCU that is used was already qualified under radiation [30] and therefore its characteristics were already known.

After the component proton beam testing, the full system was tested at the Cobalt-60 (Co60) facility at CERN. The system was tested for TID effects only, to evaluate if the combined degradation of components due to only TID would have an impact on the system. Thereafter, various radiation campaigns were performed at PSI to evaluate the lifetime of the system against all possible radiation effects on electronics, and to test and evaluate the efficiency of the mitigation scheme implemented in the MCU to cope with single event functional interrupts (SEFI). In the latest test, the system withstood 418 Gy without any degradation and without showing any SEFI. The Poisson upper-limit of the fault recoverable cross-section of the SpaceRadMon-NG was evaluated considering the uncertainty (due to the low number of event statistics) with a 95% confidence interval and was determined at $\leq 8.58 \cdot 10^{-12}$ cm^2.

IV. SYSTEM-LEVEL VALIDATION

As part of the system-level tests in the RHA approach, a test campaign at the CHARM facility was planned with two main goals. The first goal was to verify and validate the burst detection firmware which was added as mitigation in the FPGA for the error bursts introduced by the CY62157EV30LL SRAM sensor. The second goal was to demonstrate system operation and validate the system sensors in a mixed-field radiation environment that has similarities to space (on system-level) [33]. The CHARM facility is required for the test of the burst detection firmware as the particles in the facility require enough high energy to induce SEEs and error bursts in the device. The validation results of the test were positive and are presented in the next sections.

A. Methodology

For this test, the SpaceRadMon-NG was placed on the grid (G0) position in the CHARM facility. The test is a system-level approach, to test all components simultaneously and to test their mutual cooperation. CHARM provides various test positions with different flux spectra. The maximum HEH flux in the G0 position is $1.16 \cdot 10^5$ HEH $\cdot$ cm^{-2}$\cdot$s^{-1} [36]. This position was chosen to accurately study the behavior of the payload without a flux that is too high and without destroying the payload. The payload's communication signals were connected to the patch-panel in the facility through an Ethernet cable carrying the I2C signal and the clock gating signal. A separate coax cable was used to supply the power (5 V) from the patch-panel to the payload. The signals and power can be accessed in the control room above the facility. The power was supplied

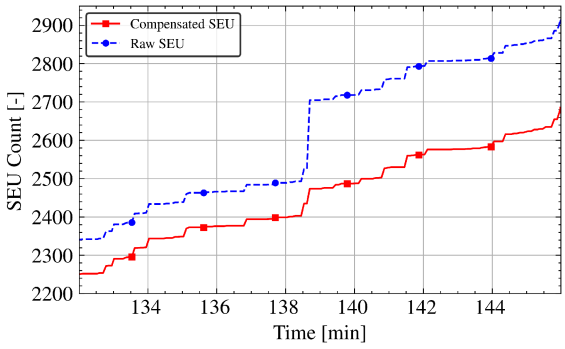

Fig. 3. Close-up of a burst event at around minute 138.5 during one of the radiation campaigns and the adequate compensation happening in the algorithm.

by an SMU set to 5 V and 100 mA current limit. The signals from the payload were picked up by a custom printed circuit board (PCB) acting as master, which contained an MCU and the required pull-ups for the I2C connection. The data were then accessed through a serial connection to a computer. This computer logged all data from the payload, as well as the data from the PSU of the voltages and currents consumed.

B. Error Burst Detection

The burst detection firmware showed its operation as intended, statistically mitigating the bursts encountered during operation. An example of the detection and mitigation of such an error burst during one of the radiation campaigns can be seen in Fig. 3. The FPGA reading is performed around every 5 seconds, with the FPGA being in sleep mode for 3 s in between readings. As seen in the figure, the algorithm implemented (explained in Section B) is effective in mitigating the error bursts. It implies that the sensor can be a reliable measurement device when this mitigation technique is implemented. The overall measurements of the HEH fluence are to be validated based on the fluence determined by the compensated SEU count and the reference sensor.

C. High Energy Hadron Fluence Measurements

The HEH fluence measurements of the CY62157 EV30LL SRAM are validated compared to the RadMon V6 system [18], a well-proven radiation monitor already used in CERN facilities. The results of this study can be seen in Fig. 4. The figure shows the fluence determined by the SEU count of the CY62157EV30LL sensor. The cross-section used was determined in a previous radiation campaign at the PIF. The figure highlights the difference between the raw SEU count of the memory and its reference (RadMon V6 memory), as well as the compatibility between the compensated SEU count and the reference used. Considering the 30% RadMon V6 uncertainty [37], depending on other experimental installations before the beam enters the CHARM facility and from the accumulation of events, the measurements can be considered compatible. The relative difference of the SpaceRadMon-NG measurement with respect to the RadMon V6 is around 0.65% over a little

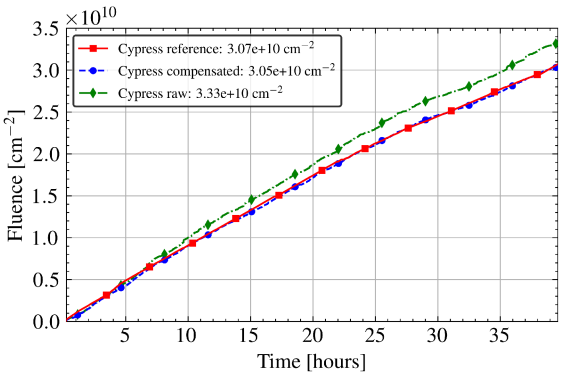

Fig. 4. HEH fluence measured by the payload SRAM over time compared to the fluence measured by the reference SRAM on the RadMon V6.

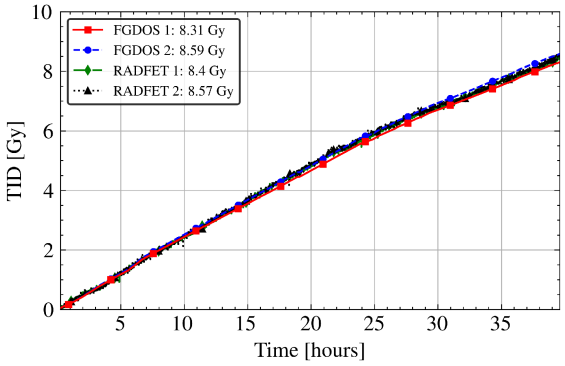

Fig. 5. TID comparison between the measurements by the FGDOS and the RADFET sensors.

less than two days and within the benchmark set, hence the sensor is validated.

D. Total Ionizing Dose Measurements

The TID sensor on the payload is the FGDOS chip, which contains two sensors able to measure the radiation. For the performance analysis, the FGDOS is compared to the current state-of-the-art RADFET integrated on the RadMon V6. In Fig. 5, the results from both sensors can be seen. Again, considering the RadMon V6 uncertainty and that the relative difference of the FGDOS measurement with respect to the RadMon V6 is on average 0.41% over a little less than two days, the measurements can be considered compatible and therefore are also validated.

The significant resolution increase is shown in Fig. 6, where the first 30 min of the radiation campaign are presented. The resolution of the FGDOS is around 2 mGy, whereas the resolution of the RADFET is much larger (around 60 mGy) giving an approximate improvement of 30 times. The resolution would be even greater if no bias voltage were applied to the RADFET. Previous studies [19] showed that the dose range, or lifetime, of the RADFET is longer by at least a factor of 2. However, as the FGDOS expected lifetime is already longer than the full system lifetime, this is not a useful characteristic.

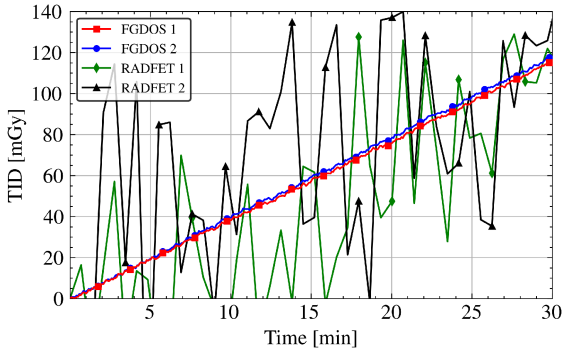

Fig. 6. TID of the FGDOS and the RADFET zoomed in on the first 30 min of the test to highlight the resolution difference.

V. FGDOS CHARACTERIZATION

Additionally to the validation of the payload, a new characterization of the FGDOS was performed using the in-house Co60 facility at CERN. This section will explain the methods used for the test and describe the results.

A. Methodology

The chip was characterized in a space-like environment, meaning undergoing simultaneous irradiation and temperature variations. The goal of the characterization was to study the evolution of the temperature coefficient in this type of environment, the sensitivity degradation and the most effective compensating method for these temperature effects [38]. The test was performed at a Co60 facility, where the temperature of the sensor was managed by a current-controlled Peltier module. The temperature profile chosen was a sinusoidal curve ranging from 23 to around 67. This higher profile was chosen to eliminate condensation problems experienced in previous tests that went below 0 °C, while still having a variation rate that is representative of space based on previous studies and measurements of on-board avionics [39], [40], [41], including the CELESTA mission. The general increase of this profile is still considered valid for the characterization, as the study purely focused on the sensor response to temperature variation. The period of the sinusoidal profile was chosen to be around 100 min, similar to the orbit duration of a satellite in LEO. For the test, three custom PCBs were used. One of the boards was the test board in active mode, undergoing temperature variations. A second control board was also in active mode but not undergoing temperature variations. A third control board was in passive mode, also not undergoing temperature variations. This setup was used to study the difference between the temperature variations in active mode and validate the active and passive modes on the control boards. This methodology can be used in future characterizations of other sensors for in space that can exhibit similar temperature and radiation responses. It is especially interesting for components that may have an enhanced degradation when undergoing the simultaneous temperature variation and irradiation or components that are highly dependent on temperature.

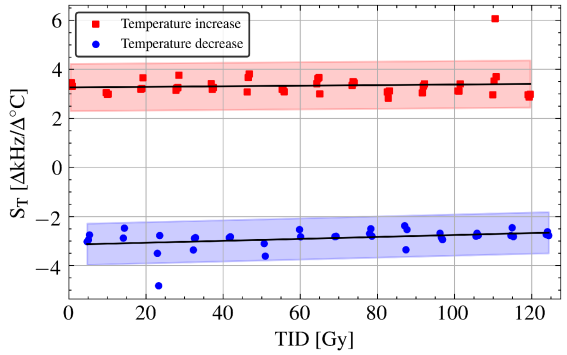

Fig. 7. Temperature coefficient evolution over the TID received of the flat region between 40 °C and 50 °C, both for increasing and decreasing temperatures.

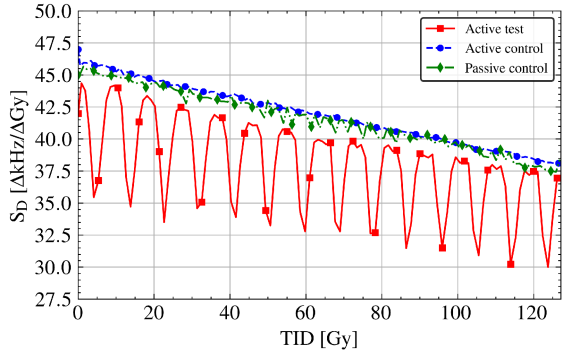

Fig. 8. Sensitivity degradation of the sensor over the TID for the different boards.

B. Temperature Coefficient Evolution

The evolution of the temperature coefficient can be seen in Fig. 7. The temperature coefficient (S_T) is determined by the change in sensor frequency (f_s) divided by the change in temperature (T), as seen in

$$S_T = \frac{\Delta f_s}{\Delta T}. \tag{1}$$

To study the evolution of the coefficient, the temperatures around the middle region of the temperature profile were taken since they have the most similar rates. The figure shows, for both positive and negative temperature variations of the FGDOS, that the temperature coefficient is constant within the transparent part, indicating the confidence intervals set at 95%.

C. Sensitivity Degradation

The sensitivity degradation was compared to what was seen in a previous study on FGDOS degradation without temperature variations [30]. From the test can be concluded that the sensitivity degradation during temperature variations was close to identical to the previous study. The main differences in sensitivity were caused by the initial sensitivity of the FGDOS sensors, which is a known characteristic of the sensor. The results of this part of the characterization can be seen in Fig. 8. It is seen that no distinction can be made between the active control and passive control board.

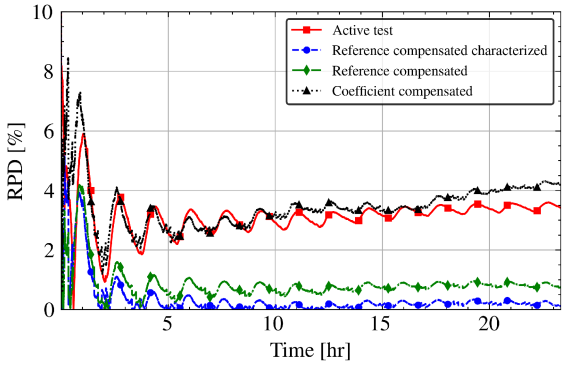

Fig. 9. RPD of the TID received of the test board with different types of temperature compensation methods and the ionization chamber. The "Active test" line is the reference without any compensation.

The active test board shows different behavior due to the temperature variations to which it is subjected. Focusing on the general trend however, which is important for the longer term, also shows indistinguishable degradation behavior compared to both control boards and the previous study. In the figure it is important to note that the device under test (DUT) in this experiment had already received 82.5 Gy, meaning the start of the degradation curve is slightly later than as seen in [30].

D. Temperature Compensation Methods

For the compensation of the temperature effects, three methods were investigated. Method 1 was based on the temperature coefficient, where the relation of the frequency to temperature was used to directly compensate for the effects. This method can be used because it was found that this coefficient stays constant over the dose received. This temperature coefficient, the same as in (1), was determined for the FGDOS using dry-runs. The coefficient was then used to determine how much sensor frequency compensation is required for the measured change in temperature. Method 2 was based on the reference frequency of a twin MOSFET that is not susceptible to TID like the floating gate, however, responds to temperature variations similarly [42]. The change in reference and sensor frequency due to temperature variations was characterized, for which the same FGDOS under test was used. A coefficient (S_f) was determined that models the behavior of the reference frequency (f_r) with respect to the sensor frequency when undergoing temperature variations, seen in the following:

$$S_f = \frac{\Delta f_s}{\Delta f_r}. \tag{2}$$

Method 3 was the same as Method 2, but the characterization from another FGDOS was used for the calculation of the required compensation. The same coefficient as in (2) was used. The results of the test can be seen in Fig. 9, where the TID is compared to the ionization chamber calibration.

Additionally to the tests, a new phenomenon was observed during the thermal dry-runs of the test set-up. While the device was undergoing temperature variations when the

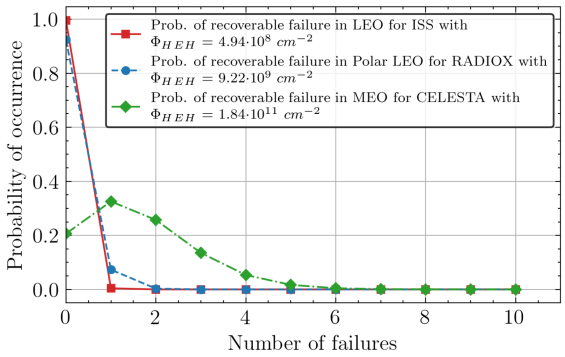

Fig. 10. Probability of self-recoverable failure is depicted for various orbits lasting 1 year with a shielding of 2 mm.

sensor frequency was close to the recharge threshold, the temperature effect could induce a recharge. This observation was made without any radiation involved and could have accuracy implications in operation like the sensor being discharged or recharged outside of the linear region of the sensor.

It can be concluded that both Method 2 and Method 3 work extremely effectively with a relative percent difference (RPD) smaller than 1% with respect to the ionization chamber used as reference. Method 1 seems to only dampen the effect of the temperature variations slightly, and it is hypothesized that this method could improve when using more accurate temperature measurements. Since Methods 2 and 3 are so close, it implies that the individual reference frequency characterization in Method 2 is not necessarily needed and Method 3 can be used to save time and effort in the future.

VI. PAYLOAD DEPENDABILITY

The OMERE 5.6 tool suite [43] was used to calculate the expected fluence in the RADIOX mission orbit, compared to other recognizable orbits such as the International Space Station (ISS) and CELESTA (the precursor mission). The RADIOX mission orbit has an approximate semimajor axis of 6939.5 km, an inclination of 97.7°, and an eccentricity of near zero. For the analysis, a shielding of 2 mm was taken with a mission life-time of one year. With the data obtained and the cross-section estimated in Section B, it is possible to estimate the probability rate of the system failure for the RADIOX mission using the homogeneous Poisson process (HPP), as has been done in [30]. This process considers a constant failure rate and independence between each failure. In Fig. 10, the probability of a recoverable fault occurring on the payload is depicted for each mission. The expected fluence for RADIOX in one year is $9.22 \cdot 10^{9}$ HEH $\cdot$ cm^{-2}. Considering the fluence expected in this mission, the probability of having 1 recoverable fault in one mission year is <7.3%. The orbit of the ISS (LEO) and CELESTA mission (MEO) have been depicted as references. Using the same mission life-time in the ISS orbit, the expected fluence during operation is $4.94 \cdot 10^{8}$ HEH $\cdot$ cm^{-2}. In this case, the probability of having 1 recoverable fault in one mission year is < 0.4%. Finally, considering the original orbit for which CELESTA was designed with a semimajor axis of 12212.2 km, inclination of 70.0°, and eccentricity of nearly 0, where the expected fluence over the same mission life-time is $1.84 \cdot 10^{11}$ HEH $\cdot$ cm^{-2}. Under these conditions, the probability of experiencing at least one recoverable fault in one mission year rises significantly (<32.6%).

It must be remembered that the SpaceRadMon-NG never exhibited any crashes during the PSI tests, and the cross-section considered was obtained using the Poisson process with 0 events. These failure rates have been evaluated considering the possible existence of a low-probability failure rate with a cross-section equal to that defined in Section B (worst case scenario). According to the test, this less probabilistic failure may not occur, and the platform should guarantee high reliability in its future use. However, in case it would, the functionalities could be restored by the OBDH through software (I2C command), hardware reset, or power cycling.

VII. CONCLUSION

The study highlights the extensive capabilities, qualifications, validations, and characterizations of the SpaceRadMon-NG payload and its sensors for space applications. The enhanced capabilities of the payload compared to the state-of-the-art are demonstrated, indicating its high versatility and ability to satisfy low-power requirements. Unique procedures and methodologies used by CERN for space applications were employed for successful qualifications and validations of both firmware and hardware, ensuring reliable operation of the payload. It ultimately resulted in the determination of the device cross-section, that being $\leq 8.58 \cdot 10^{-12}$ cm^{2} at the upper bound of the 95% confidence interval.

The COTS SRAM sensors used for HEH detection demonstrated excellent agreement with a qualified reference device, showing a relative difference of approximately 0.65% after compensation when compared to the RadMon V6 system. Similarly, the FGDOS sensor used for TID measurements exhibits a relative difference of around 0.41% with respect to the RADFET reference device. These results confirm the viability of COTS SRAM and FGDOS sensors as accurate and reliable radiation monitors, when supported by appropriate mitigation techniques. Nonetheless, the use of COTS SRAMs comes with limitations, including sensitivity to SEU bursts and micro-latchups, which require careful firmware-level handling. While the SRAMs were not characterized for temperature effects in this work, their behavior under irradiation and in representative operational modes demonstrates that they are a cost-effective and flexible option for space radiation monitoring when resource constraints are present.

A new characterization of FGDOS was conducted. The evolution of the temperature coefficient remains unchanged when irradiated, and the degradation of sensitivity exhibited indistinguishable behavior relative to its benchmark. These results imply that no additional compensation is necessary,

apart from the general temperature compensation of the frequency. The best method for this compensation was found to be the reference frequency method, where the accuracy is within 1% for the tests performed, no matter if the FGDOS being considered was characterized or not.

The payload will measure TID and HEH fluence in LEO on-board the RADIOX mission, part of the SYNDEO-1 satellite. The SpaceRadMon-NG payload can greatly enhance the understanding of the radiation environment in space, surpassing the current state-of-the-art knowledge on this topic. The results of the space missions will validate the CHARM as a system-level radiation test facility for space missions, leading to more accurate and efficient testing, qualification, and validation procedures. Furthermore, there are many possible future applications of the payload available due to its sensor versatility. It could also be employed to measure radiation levels and anticipate radiation effects on constellations. This information can then be compared with the knowledge of the satellite subsystems, so that maintenance and renewal of individual satellites in the constellation can be predicted. This operation would also give additional data on current space weather with extremely fine resolution.

REFERENCES

[1] S. Bourdarie and M. Xapsos, "The near-earth space radiation environment," *IEEE Trans. Nucl. Sci.*, vol. 55, no. 4, pp. 1810–1832, Aug. 2008.

[2] R. Ecoffet, "Overview of in-orbit radiation induced spacecraft anomalies," *IEEE Trans. Nucl. Sci.*, vol. 60, no. 3, pp. 1791–1815, Jun. 2013.

[3] A. Coronetti, "The CELESTA CubeSat in-flight radiation measurements and their comparison with ground facilities predictions," in *Proc. RADECS Conf. Inst. Elect. Electron. Eng.*, 2023, pp. 1–4.

[4] H. Koshiishi, "Space radiation environment in low earth orbit during influences from solar and geomagnetic events in december 2006," *Adv. Space Res.*, vol. 53, no. 2, pp. 233–236, Jan. 2014.

[5] R. Vainio et al., "Dynamics of the Earth's particle radiation environment," *Space Sci. Rev.*, vol. 147, no. 3/4, pp. 187–231, Nov. 2009.

[6] K. Kudela, "On energetic particles in space," *Acta Physica Slovaca*, vol. 59, no. 5, pp. 537–652, 2009.

[7] S. Svertilov et al., "Monitoring of space radiation and electromagnetic transients by Moscow state university nano-satellites," *Adv. Space Res.*, vol. 75, pp. 6608–6622, 2024.

[8] I. Fajardo et al., "Design, implementation, and operation of a small satellite mission to explore the space weather effects in LEO," *Aerospace*, vol. 6, no. 10, 2019, Art. no. 108.

[9] C. Granja et al., "The SATRAM timepix spacecraft payload in open space on board the Proba-V satellite for wide range radiation monitoring in LEO orbit," *Planet. Space Sci.*, vol. 125, pp. 114–129, Jun. 2016.

[10] H. D. R. Evans, P. Bühler, W. Hajdas, E. J. Daly, P. Nieminen, and A. Mohammadzadeh, "Results from the ESA SREM monitors and comparison with existing radiation belt models," *Adv. Space Res.*, vol. 42, no. 9, pp. 1527–1537, Nov. 2008.

[11] M. Ruffenach, S. Bourdarie, J. Mekki, D. Falguere, and J. R. Vaille, "Proton radiation belt anisotropy as seen by ICARE-NG head-A," *IEEE Trans. Nucl. Sci.*, vol. 66, no. 7, pp. 1753–1760, Jul. 2019.

[12] R. Harboe-Sorensen et al., "From the reference SEU monitor to the technology demonstration module on-board PROBA-II," *IEEE Trans. Nucl. Sci.*, vol. 55, no. 6, pp. 3082–3087, Dec. 2008.

[13] R. Harboe-Sorensen, "The technology demonstration module on-board PROBA-II," *IEEE Trans. Nucl. Sci.*, vol. 58, no. 3, pp. 1001–1007, Mar. 2011.

[14] R. Harboe-Sorensen et al., "PROBA-II technology demonstration module in-flight data analysis," *IEEE Trans. Nucl. Sci.*, vol. 59, no. 4, pp. 1086–1091, Aug. 2012.

[15] M. D'Alessio et al., "SRAMs SEL and SEU in-flight data from PROBAII spacecraft," in *Proc. RADECS Conf.*, Oxford, U.K., 2013, pp. 91–98.

[16] N. Kerboub et al., "Comparison between in-flight SEL measurement and ground estimation using different facilities," *IEEE Trans. Nucl. Sci.*, vol. 66, no. 7, pp. 1541–1547, Jul. 2019.

[17] M. Andjelkovic et al., "Design of radiation hardened RADFET readout system for space applications," in *Proc. IEEE 23rd Euromicro Conf. Digit. Syst. Des.*, 2020, pp. 484–488.

[18] G. Spiezia et al., "A new RadMon version for the LHC and its injection lines," *IEEE Trans. Nucl. Sci.*, vol. 61, no. 6, pp. 3424–3431, Dec. 2014.

[19] M. Brucoli et al., "Floating gate dosimeter suitability for accelerator-like environments," *IEEE Trans. Nucl. Sci.*, vol. 64, no. 8, pp. 2054–2060, Aug. 2017.

[20] J. Cesari, A. Barbancho, A. Pineda, G. Ruy, and H. Moser, "Floating gate dosimeter measurements at 4 M lunar flyby mission," in *Proc. IEEE Radiat. Effects Data Workshop*, 2015, pp. 1–4.

[21] R. Secondo et al., "System level radiation characterization of a 1U CubeSat based on CERN radiation monitoring technology," *IEEE Trans. Nucl. Sci.*, vol. 65, no. 8, pp. 1694–1699, Aug. 2018.

[22] J. Mekki, M. Brugger, R. Garcia Alia, A. Thornton, N. C. Dos Santos, and S. Mota, "CHARM: A mixed field facility at CERN for radiation tests in ground, atmospheric, space and accelerator representative environments," *IEEE Trans. Nucl. Sci.*, vol. 63, no. 4, pp. 2106–2114, Aug. 2016.

[23] A. Coronetti et al., "The CELESTA cubesat in-flight radiation measurements and their comparison with ground facilities predictions," *IEEE Trans. Nucl. Sci.*, vol. 71, no. 8, pp. 1623–1630, Aug. 2024.

[24] S. Danzeca et al., "Qualification and characterization of SRAM memories used as radiation sensors in the LHC," *IEEE Trans. Nucl. Sci.*, vol. 61, no. 6, pp. 3458–3465, Dec. 2014.

[25] R. Secondo et al., "Embedded detection and correction of SEU bursts in SRAM memories used as radiation detectors," *IEEE Trans. Nucl. Sci.*, vol. 63, no. 4, pp. 2168–2175, Aug. 2016.

[26] R. Secondo et al., "Analysis of SEL on commercial SRAM memories and mixed-field characterization of a latchup detection circuit for LEO space applications," *IEEE Trans. Nucl. Sci.*, vol. 64, no. 8, pp. 2107–2114, Aug. 2017.

[27] J. Prinzie, S. Thys, B. Van Bockel, J. Wang, V. De Smedt, and P. Leroux, "An SRAM-based radiation monitor with dynamic voltage control in 0.18-μm cmos technology," *IEEE Trans. Nucl. Sci.*, vol. 66, no. 1, pp. 282–289, Jan. 2019.

[28] A. Zimmaro, "FPGA - MCU design for the performance improvement of a space payload for radiation monitoring," M.Sc. thesis, Dipartimento di Ingegneria Elettrica e delle Tecnologie dell'Informazione, Naples, Italy, 2020.

[29] R. Secondo et al., "Analysis and detection of multiple cell upsets in SRAM memories used as particle detectors," in *Proc. IEEE 15th Eur. Conf. Radiat. Effects Compon. Syst.*, 2015, pp. 1–4.

[30] A. Zimmaro et al., "Testing and validation methodology for a radiation monitoring system for electronics in particle accelerators," *IEEE Trans. Nucl. Sci.*, vol. 69, no. 7, pp. 1642–1650, Jul. 2022.

[31] A. Zimmaro, R. Ferraro, J. Boch, F. Saigne, A. Masi, and S. Danzeca, "Using software mitigation schemes to improve the availability of IoT applications in harsh radiation environment," *J. Instrum.*, vol. 19, no. 2, Feb. 2024, Art. no. C02059.

[32] S. Danzeca, "Guidelines for the radiation hardness assurance (CERN-RHA) for CERN accelerators equipment," in *Proc. Int. Conf. Econ. Develop. Manage. Sci.*, 2019, Art. no. 1.

[33] A. Coronetti et al., "Radiation hardness assurance through system-level testing: Risk acceptance, facility requirements, test methodology, and data exploitation," *IEEE Trans. Nucl. Sci.*, vol. 68, no. 5, pp. 958–969, May 2021.

[34] NASA/GSFC, "Radiation effects & analysis," 2023. Accessed: Jun. 16, 2023. [Online]. Available: http://radhome.gsfc.nasa.gov

[35] C. Poivey and J. H. Day, "Radiation hardness assurance for space systems," in *Proc. IEEE NSREC Short Course*, Phoenix, AZ, USA, Jul. 2002. [Online]. Available: https://ntrs.nasa.gov/citations/20020080842

[36] A. Zimmaro et al., "Radiation test flux selection methodology to optimize see observability on systems with different operating modes," in *Proc. 22th Eur. Conf. Radiat. Effects Compon. Syst.*, 2023, pp. 1–8.

[37] G. Tsiligiannis et al., "Radiation effects on deep submicrometer SRAM-based FPGAs under the CERN mixed-field radiation environment," *IEEE Trans. Nucl. Sci.*, vol. 65, no. 8, pp. 1511–1518, Aug. 2018.

[38] J. Dijks, "Precise LEO space radiation monitoring using the Space RadMon-NG payload," M.Sc. thesis, , Dept. Space Syst. Eng., TU Delft, Delft, Netherlands, 2023.

[39] M. von Lukowicz, E. Abbe, T. Schmiel, and M. Tajmar, "Thermoelectric generators on satellites—An approach for waste heat recovery in space," *Energies*, vol. 9, no. 7, Jul. 2016, Art. no. 541.

[40] V. L. Pisacane, *Fundamentals of Space Systems*, New York, NY, USA: Oxford Univ. Press, 2005.

[41] L. Sieger, O. Nentvich, and M. Urban, "Satellite temperature measurement in LEO and improvement method of temperature sensors calibration based on the measured data," *Astronomische Nachrichten*, vol. 340, no. 7, pp. 652–657, Aug. 2019.

[42] M. Brucoli, "Total ionizing dose monitoring for mixed field environments," Ph.D. dissertation, École Doctorale Information, Structures et Systèmes (I2S), Univ. Montpellier, Montpellier, France, Nov. 2018.

[43] TRAD, "Omere download," 2025. Accessed: Mar. 29, 2025. [Online]. Available: https://www.trad.fr/en/download

Jasper Dijks was born in the Netherlands. He received the B.Sc. degree in applied physics from Eindhoven University of Technology, Eindhoven, Netherlands, in 2020, and the M.Sc. degree in aerospace engineering in 2023 from the Delft University of Technology, Delft, The Netherlands, where he is currently working toward the part-time Ph.D. degree in radiation hardness assurance of space avionics with the Space Systems Engineering Group.

As part of his M.Sc. program, he was a graduation intern with the European Organization for Nuclear Research (CERN), working on radiation testing and monitoring for space applications. He works as a Research and Development Engineer with the Royal Netherlands Aerospace Centre (NLR), where he focuses on embedded systems for space applications. He has contributed to multiple space-related projects in academia and industry. He also works on RISC-V-based flight processors and laser communication payloads for small satellites. His research interests include radiation hardness assurance, fault-tolerant computing, heterogeneous space avionics, and in situ radiation monitoring for spacecraft.

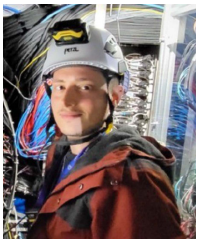

Alessandro Zimmaro received the M.Sc. degree in electronic engineering from the University of Federico II of Naples, Naples, Italy, in 2020, and the Ph.D. degree in electronic engineering from the University of Montpellier, Montpellier, France, in 2024.

He carried out his doctoral research with the European Organization for Nuclear Research (CERN), Geneva, Switzerland. His work was conducted within the framework of the radiation to electronics project (R2E) and focused on the development of a wireless application suitable for radiation environments, as well as on methodologies aimed at enhancing the radiation hardness assurance (RHA) procedures for CERN equipment. He has been with CERN since 2019 and is currently a Postdoctoral Fellow with the Electronics Production and Radiation Tolerance Section, CERN. His activities contribute to the assessment, testing, and qualification of electronic systems and components exposed to radiation in the CERN accelerator complex. His work supports the continuous improvement of radiation tolerance strategies to ensure the reliable operation of electronic infrastructure in high-energy physics environments.

Enrico Chesta received a double engineering degree from in generalist engineering (with economics option) and aerospace engineering Ecole Centrale Paris, Gif-sur-Yvette, France and Politecnico di Torino, Turin, Italy, in 1998, and an executive MBA from ESC Toulouse, Toulouse, France, in 2009.

He worked with Stanford University as a Researcher in plasma physics during 1999–2000 and with CNES (Centre National d'Etudes Spatiales) and ESA (European Space Agency) as Space Propulsion Engineer during 2001–2010, contributing to several missions (e.g., SMART-1, Microscope, Alphabus). In 2010, he joined CERN (European Organization for Nuclear Research) as leader of the Technology Transfer and IP Management Section within the Knowledge Transfer Group. He is currently CERN's Aerospace and Environmental Applications Coordinator.

Salvatore Danzeca received the Ph.D. degree in electronic engineering from the University of Montpellier, Montpellier, France, in 2015.

He received the Ph.D. degree after carrying out his studies with the European Organization for Nuclear Research (CERN), Geneva, Switzerland. His work was performed in the context of the Radiation to Electronic Project (R2E) and focused on the characterization and the qualification of the radiation sensors to embed on the radiation monitor (RadMon) for the electronics found in the CERN accelerators. He is currently the Section Leader with the Electronics Production and Radiation Tolerance Team, CERN, which is a section that includes 40 people. He is responsible for the operation, monitoring, and maintenance of more than 500 RadCon installed in the large hadron collider (LHC) and in the injector chain. He is also responsible for two radiation test facilities with CERN: CC60 (a Co60 facility) and CERN High Energy AcceleRator Mixed field/facility (CHARM). In addition, he handles the radiation testing and qualification service for COTS components in the context of CERN applications.

Dr. Danzeca is also the Chairpersonof the RADiation Working Group (RADWG), which provides support to the accelerator sector equipment groups for the assessment of the radiation tolerance of electronic equipment to be installed in radiation-exposed areas.

Rudy Ferraro was born in France. He received the master's degree in electronics with a specialization in the reliability of space systems and the Ph.D. degree in electronics from the University of Montpellier, Montpellier, France, in 2015 and 2019, respectively.

He conducted his doctoral research with CERN, where he developed radiation qualification methodologies tailored to the specific environment of the large hadron collider (LHC). He has since worked with CERN, first as a Radiation Test Engineer and currently as the Leader of the Radiation Qualification Service, responsible for the qualification of electronic components used in equipment control systems for the different particle accelerators. His research interests include radiation effects on various types of electronics, with a focus on test methodologies for optoelectronics under displacement damage, combined TID-DD effects on integrated circuits, large-scale single-event latch-up (SEL) testing, and radiation effects on FPGAs, microcontrollers, and RF systems.

Rubén García Alía (Member, IEEE) was born in Madrid, Spain, in 1986. He received a five-year degree in physics and a master's degree in applied physics from the Complutense University of Madrid, Madrid, Spain, in 2009 and 2010, respectively, and the Ph.D. degree in radiation effects in 2015 from the University of Montpellier, Montpellier, France, in collaboration with CERN, Geneva, Switzerland.

His major field of study is radiation effects in microelectronics. He is currently an Applied Physicist and Project Leader with CERN, Geneva, Switzerland. He has held previous positions as a Postdoctoral Fellow with CERN, Young Graduate Trainee with the European Space Agency (The Netherlands), and a Researcher with the Complutense University of Madrid. His work spans radiation effects testing, modeling, and radiation environment characterization for high-reliability applications in accelerators and space systems. He has led the CERN Radiation to Electronics (R2E) project since 2017, achieving major improvements in the LHC's radiation robustness. He also initiated and currently leads the RADNEXT and HEARTS EU projects, enhancing access to radiation test infrastructure and high-energy heavy ion testing capabilities, respectively. His research interests include single event effects, radiation effects testing methodologies, and the development of new simulation tools such as G4SEE and FLUKA extensions.

Dr. García Alía is a Member of NPSS and has contributed to the IEEE and RADECS communities as a Reviewer, Session Chair, Technical Chair (RADECS 2021), Deputy General Chair (RADECS 2017), and General Cochair (RADECS 2024). He served on the NPSS Radiation Effects Steering Group (2021–2024) and its Awards Committee. He received the Paul Phelps Continuing Education Grant in 2015, the RADECS 2012 Best Student Paper Award, the NSREC 2022 Meritorious Paper Award, and the 2023 IEEE Radiation Effects Early Achievement Award.

Panagiotis Gkountoumis (Member, IEEE) was born in Athens, Greece, in 1980. He received the B.Sc. degree in electronics from the University of Thessaly, Lamia, Greece, in 2005, the M.Sc. degree in control and computing from the National Technical University of Athens, Athens, Greece, in 2011, and the Ph.D. degree in physics from the National Technical University of Athens, Athens, Greece, in 2019.

In 2004, as an Undergraduate Intern, he worked on the Global Trigger Emulator System for the CMS experiment with CERN. Following his military service, where he trained as an Operator in electronic warfare, he continued working on the same project as a Researcher. In 2019, as a Postdoctoral Researcher with the University of Michigan, he contributed to the New Small Wheel upgrade of the ATLAS experiment with CERN and the Phase-II upgrade of the RPC detectors. In 2020, as a Fellow with CERN, he served as a Radiation Test Engineer and later as a Senior Engineer in board and firmware design with Boston University. He is currently based with CERN, working as a Project Scientist with the University of California, Irvine. He has authored or coauthored multiple articles in IEEE TRANSACTIONS ON NUCLEAR SCIENCE, *Nuclear Instruments*, and *ResearchGate*.

Dr. Gkountoumis has also served as a Reviewer for IEEE TRANSACTIONS ON NUCLEAR SCIENCE.

Alessandro Masi received the M.S. degree in electronic engineering and the Ph.D. degree in computer science from the University of Naples Federico II, Naples, Italy, in 2001 and 2005, respectively.

His Ph.D. research was carried out with the Magnetic Measurements and Tests Group, CERN, Geneva, Switzerland, on high-accuracy measurement systems for the superconducting magnets of the large hadron collider. In 2005, he was a Staff Member with the Sources, Targets, and Interactions Group, CERN. In 2008, he was a Section Leader with the Equipment Controls and Electronics Section, CERN. Since 2018, he has been the Lead of the Survey, Mechatronics and Measurements Group, CERN.

Alessandra Menicucci received the laurea degree in experimental particle physics from the University of Rome La Sapienza, Rome, in 2000, and the Ph.D. degree in physics from the University of Rome Tor Vergata, Rome, Italy, in 2004.

She is currently an Associate Professor with the Space Systems Engineering Section, Aerospace Engineering Faculty, Delft University of Technology, Delft, The Netherlands. From 2006 to 2015, she worked with the European Space Agency, Space Environment and Effects Section, where she was responsible for several space radiation monitoring developments. She also supported various ESA missions in space environment and effects analysis, including Giove-B, GOCE, Alphasat, MetOp, Proba-V, EuTEF, and JUICE. She is currently the Program Manager with the Delfi Space Program, which aims to advance education and research through the end-to-end engineering of space missions with high relevance and impact, using very small satellites. Previous missions include the CubeSats Delfi-C3 (2008) and Delfi-n3Xt (2013), as well as the picosatellite Delfi-PQ, launched in January 2022. She also manages the Space Lab, Faculty of Aerospace Engineering, Delft University of Technology. She is the (co)author of more than 60 refereed journal and conference papers. She has cosupervised three Ph.D. candidates and is currently supervising three more as promotor. She is also a coinvestigator in several national and international projects in the field of radiation hardness assurance for miniaturized systems. Her research interests include the development of miniaturized space systems that can be distributed onboard micro-satellites, as well as the analysis of the space radiation environment and its effects.

Jeffrey Prinzie (Member, IEEE) received the M.Sc. degree in microelectronics and Ph.D. degree in electrical engineering from Katholieke Universiteit Leuven (KU Leuven), Leuven, Belgium, in 2013 and 2017, respectively.

During his Ph.D. degree, he has worked on radiation-tolerant integrated circuits with the ADVISE Research Group, Department of Electrical Engineering (ESAT), KU Leuven, on the hardening of time-based mixed-signal circuits, especially PLLs and TDCs. In 2017, he continued his Postdoctoral research. From 2018 to 2019, he has worked as a Visiting Researcher with MediaTek, U.K., on ultrafast locking all-digital synthesizers for reliable 5 G communication systems. Since 2020, he has been an Assistant Professor with KU Leuven, where he is focusing on highly digital integrated circuits such as fast time-to-digital converters, fault-tolerant digital implementations, and digitally assisted communication systems for harsh environments.